Supplementary Material: Nonequilibrium mode-coupling theory for the steady state of dense active systems of self-propelled particles

Saroj Kumar Nandi[1,*] and Nir S. Gov[2]

[1]*Department of Materials and Interfaces, Weizmann Institute of Science, Rehovot 7610001, Israel*
[2]*Department of Chemical Physics, Weizmann Institute of Science, Rehovot 7610001, Israel*

In this Supplementary Material, we provide some discussion of the active system, details of the schematic MCT calculation, a brief description of the numerical method and some results of the equilibrium mode-coupling theory that are relevant for our discussion.

SI. Description of active systems of self-propelled particles

We consider an active system of self-propelled particles in the dense regime. Each particle has a self-propulsion force f_0 and persistence time τ_p for its motion in a certain direction, which is marked by an arrow on the particles in Fig. S1 for clarity. The fact that dynamics of such a system is different from a passive system can be understood from the following simple consideration. Let us consider one collision event between two particles as shown in the right of Fig. S1. As the particles approach towards each other, imagine the directors point towards each other as shown in the figure. As they collide, they move away from each other due to the short-range repulsive potential, but, because their self-propulsion remains along their directors, they again move towards each other and collide. This continues over a timescale of the order of τ_p, until the directors loose their correlation. Thus, even if the particles are purely repulsive, self-propulsion that is persistent for a timescale of τ_p, creates an effective attractive force among the particles. In our description, we implement activity through the active noise statistics. Usually two such statistics have been considered in the literature [1, 2] as we discuss in the main text.

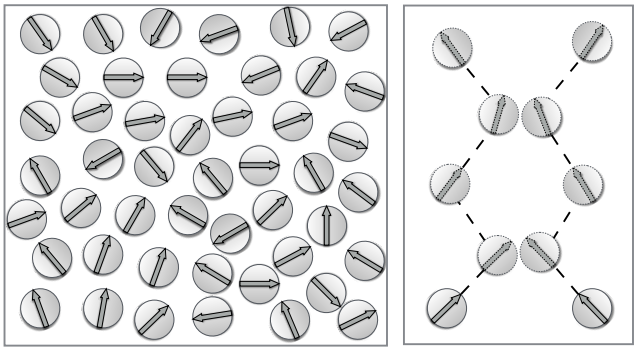

FIG. S1: Schematic picture of an active system consisting of self-propelled particles with a self-propulsion force f_0 and persistence time τ_p for their motion in a certain direction. One possible effect of persistence is schematically illustrated in the right on a collision event of two particles (see text for details).

*Electronic address: saroj.nandi@weizmann.ac.il

SII. Mode-coupling theory

Mode-coupling theory (MCT) [3–5] was developed in the early 80's for studying the complex behaviour when a fluid is supercooled or its density increases. The viscosity and relaxation time of the fluid in this regime increases by 10-12 orders of magnitude for a modest change in temperature (or density). MCT provides an intuitive and powerful mechanism to understand this rapid change in the transport coefficients through a non-linear feedback mechanism. Ref. [6] presents an instructive explanation of this feedback mechanism where the structure of the fluid depends on its viscosity which in turn is determined via the structure itself. Despite being one of the most popular theories in the field of glassy dynamics [7], a clear understanding of the theory, and its key ingredients, still remains illusive and often spiritedly debated to this date. There are a number of ways to derive the theory: the projection operator formalism [4, 5], starting with the Newton's equations of motion for individual particles [8], the hydrodynamic approach [3, 9, 10], the field theoretic method [5, 11], etc are some of the examples.

MCT assumes that the statics of the system is already known, and taking the static properties as inputs, the theory gives the dynamics of the system. The theory provides an equation of motion of the two-point dynamic correlation function that we must solve numerically as an initial value problem since the equation is a nonlinear integro-differential equation and no general analytical solution is known. It requires the inputs of the static structure factor (S_k) and the direct correlation function (c_k); these two quantities are related in equilibrium as $S_k = 1/(1-\rho_0 c_k)$, where ρ_0 is the average density. Thus, once we know either of S_k or c_k from experiment, simulation or other theories, MCT provides the time-evolution of the dynamic structure factor and this can be used to calculate different transport coefficients like the viscosity or relaxation time. In scenarios where the solution of the full wave vector dependent theory becomes intractable [12], one often takes a schematic approximation [13] throwing away all wave vector dependence but

one (corresponding to the first maxima of S_k) and obtains the schematic MCT. Within this limit, the input to the theory simply becomes a number λ. The schematic MCT retains the main mechanism of the theory and is quite useful for insights.

SIII. Details of the mode-coupling theory calculation

We have the full wavevector-dependent equations of motion for the correlation, $C_k(t,t') = \langle \delta\rho_k(t)\delta\rho_{-k}(t')\rangle$, and the response, $R_k(t,t') = \langle \partial\delta\rho_k(t)/\partial \hat{f}_T^L(t')\rangle$, functions (Eqs (7-9) in the main text):

$$\frac{\partial C_k(t,t')}{\partial t} = -\mu_k(t)C_k(t,t') + \int_0^{t'} \mathrm{d}s\mathcal{D}_k(t,s)R(t',s) + \int_0^t \mathrm{d}s\Sigma_k(t,s)C_k(s,t') + 2TR_k(t',t) \tag{S1}$$

$$\frac{\partial R_k(t,t')}{\partial t} = -\mu_k(t)R_k(t,t') + \int_{t'}^t \mathrm{d}s\Sigma_k(t,s)R_k(s,t') + \delta(t-t') \tag{S2}$$

$$\mu_k(t) = TR_k(0) + \int_0^t \mathrm{d}s[\mathcal{D}_k(t,s)R_k(t,s) + \Sigma_k(t,s)C_k(t,s)] \tag{S3}$$

with

$$\mathcal{D}_k(t,s) = \frac{\kappa_1^2}{2}\int_{\mathbf{q}} \mathcal{V}_{k,q}^2 C_q(t,s)C_{k-q}(t,s) + \kappa_2^2\mathcal{D}_k(t-s), \tag{S4}$$

$$\Sigma(t,s) = \kappa_1^2 \int_{\mathbf{q}} \mathcal{V}_{k,q}^2 C_{k-q}(t,s)R_q(t,s), \tag{S5}$$

where $\kappa_1 = k_BT/D_Lk^2$ and $\kappa_2 = 1/D_L$. The details of this field-theoretical method can be found in a number of places, including [5, 14, 15]. Eqs. (S1-S5) form the mode-coupling theory for a generic nonequilibrium non-stationary state of an active system. However, the numerical solution of these equations is not possible due to excessive time-requirement with the currently available algorithms, even in the steady-state limit, where we need to solve the equations iteratively (see Sec. SV). We therefore take a schematic approximation, writing the theory at a particular wave vector k_{max}, which corresponds to the first maximum of the static structure factor, that leads to simplified equations manageable for numerical solution. Then we obtain the equations for

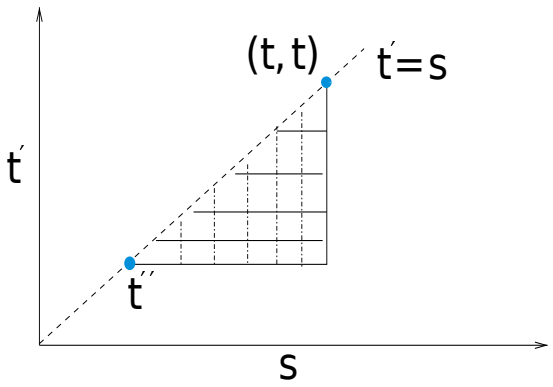

FIG. S2: Region of integration for the last term in Eq. (S10). We need to change the order of integration for the variables t' and s to obtain Eq. (S11) [see text].

$C(t,t') \equiv C_{k=k_{max}}(t,t')$ and $R(t,t') \equiv R_{k=k_{max}}(t,t')$ as

$$\frac{\partial C(t,t')}{\partial t} = -\mu(t)C(t,t') + \int_0^{t'} \mathrm{d}s\mathcal{D}(t,s)R(t',s) + \int_0^t \mathrm{d}s\Sigma(t,s)C(s,t') + 2TR(t',t) \tag{S6}$$

$$\frac{\partial R(t,t')}{\partial t} = -\mu(t)R(t,t') + \int_{t'}^t \mathrm{d}s\Sigma(t,s)R(s,t') + \delta(t-t') \tag{S7}$$

$$\mu(t) = T + \int_0^t \mathrm{d}s[\mathcal{D}(t,s)R(t,s) + \Sigma(t,s)C(t,s)] \tag{S8}$$

with $\mathcal{D}(t,s) = 2\lambda C^2(t,s) + \Delta(t-s)$ and $\Sigma(t,s) = 4\lambda C(t,s)R(t,s)$. Note that λ contains the information of interaction through the direct correlation function. It is well-known that the schematic form of MCT and the equations for p-spin glass model are analogous [16] and similar equations, as in Eqs. (S6-S8), were also obtained in [17] for the p-spin spherical active spin glass model. Now we define the integrated response function $F(t,t')$ as

$$F(t,t') = -\int_{t'}^t R(t,s)\mathrm{d}s, \tag{S9}$$

as this is more advantageous for the numerical integration since R fluctuates more compared to F. To write the equations in terms of $F(t,t')$, we take an integration of Eq. (S7) on t' and obtain

$$\frac{\partial F(t,t'')}{\partial t} = -\mu(t)F(t,t'') - 1 - \int_{t''}^t \int_{t'}^t \mathrm{d}s\Sigma(t,s)R(s,t')\mathrm{d}t'. \tag{S10}$$

We show the region of integration for the last term above in Fig. S2 where we need to do the integration for s first and then on t'. However, to write the equation in terms of $F(t,t')$, we need to carry out the integration on t' first (i.e., along the dotted lines), when the integration limits go from t'' to s. Then we obtain the equation for $F(t,t')$

from Eq. (S7) as

$$\frac{\partial F(t,t')}{\partial t} = -1 - \mu(t)F(t,t') + \int_{t'}^{t} \mathrm{d}s \Sigma(t,s)F(s,t'). \tag{S11}$$

Using the definitions of $\mathcal{D}(t,t')$ and $\Sigma(t,t')$ in Eqs. (S6-S8) we obtain the equations of motion for the correlation, $C(t,t')$, and integrated response, $F(t,t')$, functions as

$$\begin{aligned}\frac{\partial C(t,t')}{\partial t} &= -\mu(t)C(t,t') + 2\lambda \int_0^{t'} \mathrm{d}s C^2(t,s)\frac{\partial F(t',s)}{\partial s} \\ &+ 4\lambda \int_0^{t} \mathrm{d}s C(t,s)\frac{\partial F(t,s)}{\partial s}C(s,t') \\ &+ \int_0^{t'} \Delta(t-s)\frac{\partial F(t',s)}{\partial s}\mathrm{d}s \end{aligned} \tag{S12a}$$

$$\begin{aligned}\frac{\partial F(t,t')}{\partial t} &= -1 - \mu(t)F(t,t') \\ &+ 4\lambda \int_{t'}^{t} \mathrm{d}s C(t,s)\frac{\partial F(t,s)}{\partial s}F(s,t') \end{aligned} \tag{S12b}$$

$$\begin{aligned}\mu(t) =& T + \int_0^t \mathrm{d}s \left[\left\{ 2\lambda C^2(t,s) + \Delta(t-s) \right\} \frac{\partial F(t,s)}{\partial s} \right. \\ &\left. + 4\lambda C(t,s)\frac{\partial F(t,s)}{\partial s}C(t,s) \right] \end{aligned} \tag{S12c}$$

These equations are valid in general for a non-equilibrium system even in the aging regime. We assume that the system goes to a steady state at long time and $C(t,t')$ and $F(t,t')$ become functions of the time difference $(t-t')$ alone. It can be shown through the numerical solution of Eqs. (S12) that if the final parameter values are such that the system is in liquid state, the system dynamically evolves to this steady state. To obtain the equations for this steady state, we take the limits of t and t' to ∞ such that $(t-t') = \tau$ remains finite. Then, we obtain

$$\begin{aligned}\frac{\partial C(\tau)}{\partial \tau} &= \Pi(\tau) - \mu(\infty)C(\tau) - \epsilon(\tau) \\ &+ 4\lambda \int_0^{\tau} \mathrm{d}s C(\tau - s)\frac{\partial F(\tau - s)}{\partial s}C(s) \end{aligned} \tag{S13}$$

$$\frac{\partial F(\tau)}{\partial \tau} = -1 - \mu(\infty)F(\tau) - 4\lambda \int_0^{\tau} \mathrm{d}s C(s)\frac{\partial F(s)}{\partial s}F(\tau - s)$$

where the different parameters are defined as

$$\Pi(\tau) = -\int_{\tau}^{\infty} \Delta(s)\frac{\partial F(s-\tau)}{\partial s}\mathrm{d}s \tag{S14a}$$

$$\begin{aligned}\epsilon(\tau) &= 2\lambda \int_{\tau}^{\infty} \mathrm{d}s C^2(s)\frac{\partial F(s-\tau)}{\partial s} \\ &+ 4\lambda \int_{\tau}^{\infty} \mathrm{d}s C(s)\frac{\partial F(s)}{\partial s}C(s-\tau) \end{aligned} \tag{S14b}$$

$$\mu(\infty) = T - 6\lambda \int_0^{\infty} \mathrm{d}s C^2(s)\frac{\partial F(s)}{\partial s} - \int_0^{\infty} \Delta(s)\frac{\partial F(s)}{\partial s}\mathrm{d}s. \tag{S14c}$$

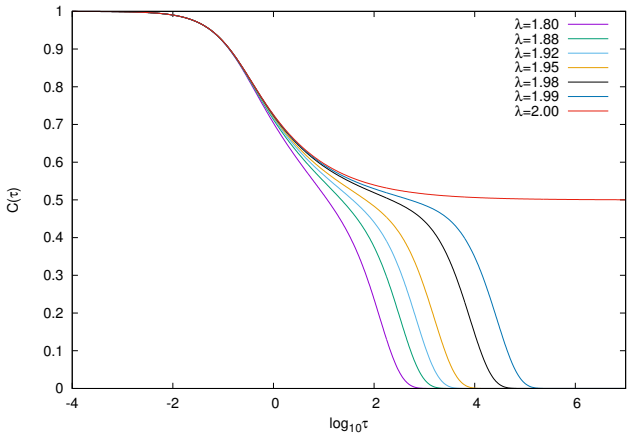

FIG. S3: Decay of the correlation function $C(\tau)$ for different values of λ within equilibrium MCT obtained from solving Eq. (S16). $C(\tau)$ doesn't decay to zero for $\lambda \geq 2.0$ and this is the MCT transition when the system goes to a non-ergodic state. We note that the non-ergodic state is not found in simulation or experiments where some other mechanisms, absent within MCT, takes over and the theory fails to describe the system beyond this point.

In equilibrium, considering the fluctuation-dissipation relation (FDR), such that $\partial C/\partial\tau = T\partial F/\partial\tau$, we obtain the equation for the correlation function from Eq. (S13) as

$$\begin{aligned}\frac{\partial C(\tau)}{\partial \tau} + TC(\tau) + \frac{2\lambda}{T}C^3(\infty)[1 - C(\tau)] \\ + \frac{2\lambda}{T}\int_0^{\tau} C^2(\tau - s)\frac{\partial C(s)}{\partial s}\mathrm{d}s = 0. \end{aligned} \tag{S15}$$

This equation becomes the standard MCT equation for the ergodic state when $C(\infty) = 0$ and the third term in the above equation vanishes. But in the nonergodic state, $C(\infty)$ is non-zero and Eq. (S15) is different from the standard MCT equation. A resolution of this paradox has been offered in [18], where it has been shown that to obtain the MCT from the field-theoretic treatment in the non-ergodic state, one must start from a different initial condition that is commensurate to this state and then one obtains the standard MCT equation. We concentrate on the ergodic state in this work where $C(\infty) = 0$ and obtain the equilibrium MCT equation as

$$\frac{\partial C(\tau)}{\partial \tau} + TC(\tau) + \frac{2\lambda}{T}\int_0^{\tau} C^2(\tau - s)\frac{\partial C(s)}{\partial s}\mathrm{d}s = 0. \tag{S16}$$

The solution of Eq. (S16) is well known [3, 4]. We set T to unity and show the decay of $C(\tau)$ as a function of $\log\tau$ for different values of λ in Fig. S3. As λ increases, the decay of $C(\tau)$ becomes slower and at $\lambda = 2.0$, $C(\tau)$ doesn't decay to zero anymore, this is the MCT transition point where the system goes to a non-ergodic state. Such a transition, however, is not found in simulations or experiments on structural glasses and the theory fails to

describe the system beyond this point. Within this description, λ is inversely proportional to T and therefore, in terms of T, larger λ can be seen as results for small T.

Eqs. (S13) along with the definitions in (S14) give the mode-coupling theory for an active system of self-propelled particles in the dense or low temperature regime. A closer look at Eqs. (S14) shows that evaluation of the variables $\Pi(\tau)$, $\epsilon(\tau)$ and $\mu(\infty)$ requires the values of $C(\tau)$ and $F(\tau)$ for all values of τ, from 0 to ∞. Therefore, we must solve the equations through an iterative method, and the algorithm must be extremely accurate. We have modified the algorithm that was used to investigate the aging behavior in [12] for a steady state. However, this algorithm is not extremely accurate close to the transition and a small error gets amplified at later iterations and the solution blows up. To give an example, when $T = 1.0$ and $\lambda = 1.99$, we could not iterate the solution for more than thrice. Therefore, we write the equations slightly differently using a generalized FDR through the definition of a time-dependent effective temperature $T_{eff}(\tau)$

$$\frac{\partial C(\tau)}{\partial \tau} = T_{eff}(\tau)\frac{\partial F(\tau)}{\partial \tau}. \tag{S17}$$

We have seen that $T_{eff}(\tau)$, obtained through Eq. (S17) from the numerical solution of Eqs. (S13), varies slowly and has two distinct regime as discussed in the main text. At small τ, $T_{eff}(\tau) = T$ and at large τ it goes to a different value, larger than T and the crossover from T to the larger value occurs at a timescale $\tau \sim \mathcal{O}(\tau_p)$. Therefore, we are justified to assume that $T_{eff}(\tau)$ varies slowly and write the MCT equations for the active steady state as

$$\frac{\partial C(\tau)}{\partial \tau} = \Pi(\tau) - (T-p)C(\tau) - \int_0^\tau m(\tau-s)\frac{\partial C(s)}{\partial s}\mathrm{d}s \tag{S18}$$

$$\frac{\partial F(\tau)}{\partial \tau} = -1 - (T-p)F(\tau) - \int_0^\tau m(\tau-s)\frac{\partial F(s)}{\partial s}\mathrm{d}s \tag{S19}$$

where we have

$$m(\tau-s) = 2\lambda\frac{C^2(\tau-s)}{T_{eff}(\tau-s)} \tag{S20a}$$

$$p = \int_0^\infty \Delta(s)\frac{\partial F(s)}{\partial s}\mathrm{d}s \tag{S20b}$$

$$\Pi(\tau) = -\int_\tau^\infty \Delta(s)\frac{\partial F(s-\tau)}{\partial s}\mathrm{d}s. \tag{S20c}$$

Note that the definition of $T_{eff}(\tau)$ through Eq. (S17) doesn't imply any loss of generality as we evaluate $T_{eff}(\tau)$ at each time step. The advantage of the above form is that the standard algorithm, that can be used with large accuracy, for equilibrium MCT can be easily extended and used through an iteration method, as discussed in Sec. SV, therefore we chose to present the theory in the form of Eqs. (S18-S20). We have checked

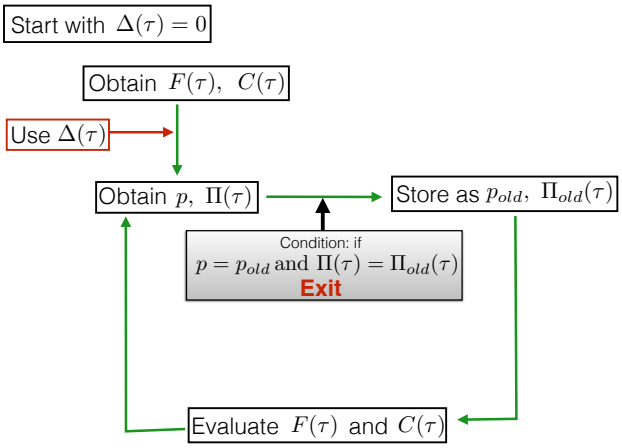

FIG. S4: Illustration of the iterative procedure for the solution of the mode-coupling theory for the steady-state of an active system.

that in the regime of parameter space, where the earlier numerical method works, the solutions of Eqs. (S13-S14) and Eqs. (S18-S20) are the same. The initial conditions for the correlation and response functions are $C(0) = 1.0$ and $F(0) = 0.0$.

SIV. Details of the STAP model

As we discussed in the main text, the scenario of a single trapped active particle (STAP) in a harmonic potential is valid at short to intermediate time scales, particularly around the α-relaxation regime of MCT. We consider the Langevin equation for the dynamics of a single particle as [19]

$$m\ddot{x}(t) = -U'(x) - \gamma\dot{x}(t) + \eta(t) + f(t) \tag{S21}$$

where m is the mass of the particle, γ, the effective friction force, $\eta(t)$, the thermal noise with zero mean and $\langle\eta(t)\eta(t')\rangle = 2k_BT\gamma\delta(t-t')$ and $f(t)$, the active noise with zero mean. We have considered two different statistics for the active noise:

$$\text{SNTC statistics: } \langle f(t)f(0)\rangle = \Delta_0 \exp[-t/\tau_p] \tag{S22}$$

$$\text{OUP statistics: } \langle f(t)f(0)\rangle = \frac{T^{sp}_{eff}}{\tau_p}\exp[-t/\tau_p], \tag{S23}$$

where both Δ_0 and T^{sp}_{eff} are proportional to the square of the active force amplitude: f_0^2. We ignore the acceleration term as we are looking at the glassy regime, where this term is not important. We consider the harmonic potential $U(x) = kx^2/2$. Then we obtain

$$k\langle x(t)^2\rangle = k_BT + \frac{H\Theta}{1+G\tau_p}, \tag{S24}$$

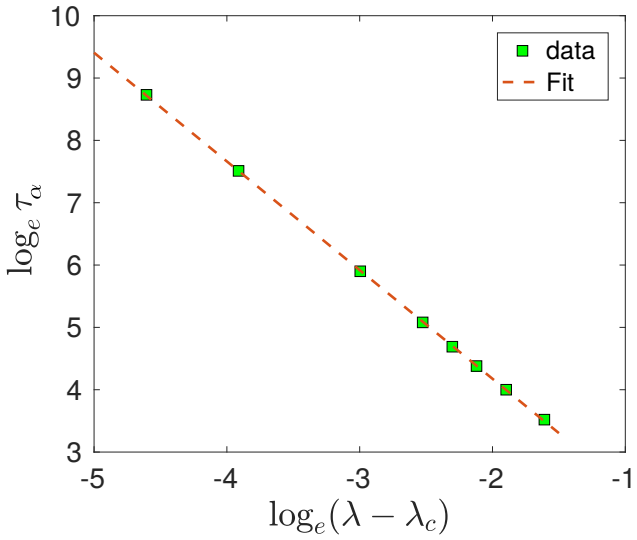

FIG. S5: Symbols are the equilibrium MCT data of τ_α when the correlation function $C(\tau)$ becomes 0.4 (see Fig. S3). The dashed line is a fit to the equation $\log \tau = a - \gamma \log(\lambda - \lambda_c)$ with $a = 0.69$ and $\gamma = 1.74$.

where $H = 1/2\gamma$, $G = k/\gamma$, $\Theta = \Delta_0 \tau_p$ for SNTC statistics and $\Theta = T_{eff}^{sp}$ for OUP model. Eq. (S24) gives the mean potential energy of the particle. In Ref. [19], it was shown that this energy is related to the spatial extent over which there is a non-zero probability of finding the particle. Therefore, this energy should be related to the probability of a particle to move to the edge of the cage and escape from it. In other words, this energy should be related to the FDR ratio that MCT provides in the α-relaxation regime, where the particle comes out of the cage formed by neighboring particles and we relate this to the effective temperature $T_{eff}(\tau \to \infty) \equiv T_{eff}$ defined in the main text. For the two models we therefore have:

$$T_{eff} = \begin{cases} T + \frac{H\Delta_0\tau_p}{1+G\tau_p}, & \text{for SNTC statistics} \\ T + \frac{HT_{eff}^{sp}}{1+G\tau_p}, & \text{for OUP statistics.} \end{cases} \quad \text{(S25)}$$

From the numerical solution of active MCT [Eqs. (S18-S20)], we see $T_{eff}(\tau) = T$ at very short timescale and saturates to a larger value at long time (see main text). $T_{eff}(\tau \to \infty)$ agrees well with Eq. (S25) as we show in the main text.

SV. Numerical Solution

The numerical solution of Eqs. (S18-S19) along with the definitions in Eqs. (S20) can be obtained through a generalization of the standard algorithm to solve the MCT equations in equilibrium [20–22]. The advantage of this algorithm is that it can be used with any desired accuracy simply through the reduced initial step size and increasing the number of steps after which the time-step is doubled [21]. We start with the passive system at a certain T and λ with $\Delta(\tau) = 0$ and obtain $C(\tau)$ and $F(\tau)$. $T_{eff}(\tau)$ for $\Delta(\tau) = 0$ is equal to T. We then use these values of $F(\tau)$ to obtain p and $\Pi(\tau)$ using the relations in Eqs. (S20). We again evaluate $C(\tau)$ and $F(\tau)$ with these new values of parameters and obtain these parameters again with the new values of $F(\tau)$. We continue this process until the older and new values of p and $\Pi(\tau)$ are same. We illustrate this through a flowchart in Fig. S4. When activity is not very large (for example $\Delta_0 = 0.1$ and $\tau_p = 0.1$), it takes around 30 iterations to achieve the desired accuracy, however, for larger activity parameters, it takes of the order of 100 iterations for the solution to converge.

SVI. Exponent for the power-law divergence of α-relaxation time within schematic MCT

In a glassy system, we are interested in the long time dynamics and therefore we look at the α-relaxation time τ_α that is defined as the time when $C(\tau)$ becomes 0.4. We obtain the mode-coupling exponent γ for the α-relaxation time with $\tau_\alpha \sim (\sigma - \sigma_c)^{-\gamma}$, where σ is any control parameter (T or density) and σ_c is its critical value where we obtain the MCT transition for the passive system.

We extract τ_α from the numerical solution of Eq. (S16), and fit the data with a form $\log \tau = a - \gamma \log(\lambda - \lambda_c)$ and obtain $a = 0.69$ and $\gamma = 1.74$. In simulations or experiments, this value of γ may vary slightly, as is well-known for the equilibrium MCT, however, what is important is that the same exponent for the passive system governs the effect of activity on the dynamics of the active system when the parameters are such that the passive system is close to the MCT transition point.

[1] E. Flenner, G. Szamel, and L. Berthier, Soft Matter **12**, 7136 (2016).
[2] R. Mandal, P. J. Bhuyan, M. Rao, and C. Dasgupta, Soft Matter **12**, 6268 (2016).
[3] S. P. Das, Rev. Mod. Phys. **76**, 785 (2004).
[4] W. Götze, *Complex Dynamics of Glass-Forming Liquids: A Mode-Coupling Theory* (Oxford University Press, Oxford, 2008).
[5] D. R. Reichman and P. Charbonneau, J. Stat. Mech.: Theor. Expt. p. P05013 (2005).
[6] T. Geszti, J. Phys. C: Solid State Phys. **16**, 5805 (1983).
[7] L. Berthier and G. Biroli, Rev. Mod. Phys. **83**, 587 (2011).
[8] E. Zaccarelli, G. Foffi, P. D. Gregorio, F. Sciortino,

P. Tartaglia, and K. A. Dawson1, J. Phys.: Condens. Matter **14**, 2413 (2002).
[9] K. Kawasaki, J. Stat. Phys. **110**, 1249 (2002).
[10] S. K. Nandi, S. M. Bhattacharyya, and S. Ramaswamy, Phys. Rev. E **84**, 061501 (2011).
[11] K. Miyazaki and D. R. Reichman, J. Phys. A: Math. Gen. **38**, L343 (2005).
[12] S. K. Nandi and S. Ramaswamy, Phys. Rev. Lett. **109**, 115702 (2012).
[13] E. Leutheusser, Phys. Rev. A **29**, 2765 (1984).
[14] T. Castellani and A. Cavagna, J. Stat. Mech.: Theor. Expt. p. P05012 (2005).
[15] S. K. Nandi and S. Ramaswamy, Phys. Rev. E **94**, 012607 (2016).
[16] T. R. Kirkpatrick and D. Thirumalai, Phys. Rev. Lett. **58**, 2091 (1987).
[17] L. Berthier and J. Kurchan, Nat. Phys. **9**, 310 (2013).
[18] A. Barrat, R. Burioni, and M. Mézard, J. Phys. A: Math. Gen. **29**, L81 (1996).
[19] E. Ben-Isaac, É. Fodor, P. Visco, F. van Wijland, and N. S. Gov, Phys. Rev. E **92**, 012716 (2015).
[20] M. Fuchs, W. Gotze, I. Hofacker, and A. Latz, J. Phys.: Condens. Matter **3**, 5047 (1991).
[21] K. Miyazaki, B. Bagchi, and A. Yethiraj, J. Chem. Phys. **121**, 8120 (2004), note that an earlier version, and not the published one, of this paper (available in arXiv:cond-mat/0405326v1) contains the details of the algorithm.
[22] E. Flenner and G. Szamel, Phys. Rev. E **72**, 031508 (2005).